Chapter 2
Hydrolysis of Cellulose to Glucose Using Carbon Catalysts

2.1 Introduction

Cellulose is a potential and attractive alternative to petrol to reduce emission of greenhouse gases as this plant-derived biomass resource is an abundant, non-food, and renewable carbon source [1–6]. Glucose, a monomer of cellulose, is a key intermediate of various useful chemicals such as polymers, medicines, surfactants, gasoline, and diesel fuels (Sect. 1.2.3) [7–9]. Accordingly, the reaction of cellulose to glucose (Fig. 2.1) will be a mainstream in the next-generation biorefinery, which will substitute current processes using food biomass. However, realizing this vision has been hampered by the recalcitrance of cellulose and various practical difficulties as described in Chap. 1.

The hydrolysis of cellulose has been performed with various solid catalysts, as heterogeneous catalysts are advantageous over homogeneous ones in terms of easy separation from products [6, 10–12]. In the previous works, it was found that unmodified mesoporous carbon CMK-3 catalyzed the hydrolysis of cellulose [13, 14]. Fukuoka et al. has proposed that the active sites of CMK-3 would be weakly acidic groups [14]. Due to the absence of strong acid sites, CMK-3 stands in stark contrast to sulfonated carbons [15, 16] that have been widely studied in the hydrolysis of cellulose. Sulfonated catalysts possibly suffer from the leaching of SO_3H groups in hot compressed water [17], whereas weakly acidic carbons such as CMK-3 are expected to be highly hydrothermally stable. Furthermore, salts included in raw biomass easily deactivate strong acids by ion exchange; in contrast, weak acids potentially preserve their catalytic activities even in the presence of salts [18, 19]. These great advantages of weakly acidic carbons potentially break through the barrier of practical hydrolysis of cellulosic biomass. However, the highest glucose yield obtained by CMK-3 was only 16 %, and the synthesis of CMK-3 [20] was complicated in the practical perspective. Hence, in this chapter, the author has aimed the high-yielding synthesis of glucose from cellulose and real cellulosic biomass using more common carbon materials.

M. Yabushita, *A Study on Catalytic Conversion of Non-Food Biomass into Chemicals*, Springer Theses, DOI 10.1007/978-981-10-0332-5_2

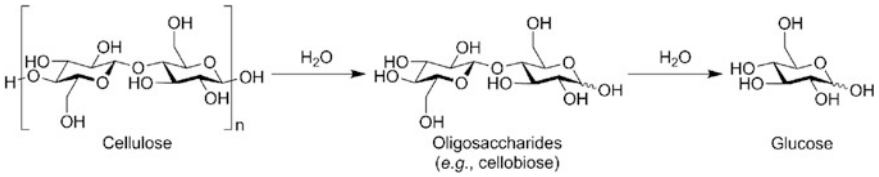

Fig. 2.1 Hydrolysis of cellulose to glucose via oligosaccharides

2.2 Experimental

2.2.1 Reagents

Microcrystalline cellulose	Column chromatography grade, 102331, Merck
Bagasse kraft pulp	Harvested in Okinawa Prefecture in Japan, composition determined by the established method (see Sect. 2.2.4) [21]: cellulose (59 wt%), hemicellulose [27 wt% (xylan 25 wt%, arabinan (2 wt%)], and lignin (9 wt%), Showa Denko
K26	Alkali-activated carbon (not for sale), Showa Denko
K20	Alkali-activated carbon (not for sale), Showa Denko
MSP20	Alkali-activated carbon, Kansai Coke & Chemicals
BA50	Steam-activated carbon, Ajinomoto Fine Techno
SX Ultra	Steam-activated carbon, Norit, denoted as SX
Vulcan XC72	Carbon black, Cabot, denoted as XC72
Black Pearls 2000	Carbon black, Cabot, denoted as BP2000
Pluronic P123	Triblock copolymer, $HO(CH_2CH_2O)_{20}(CH_2CH(CH_3)O)_{70}(CH_2CH_2O)_{20}H$, Sigma-Aldrich
Tetraethyl orthosilicate	>99.0 %, Sigma-Aldrich, denoted as TEOS
Ethanol	Special grade, Wako Pure Chemical Industries
Sulfuric acid	96–98 %, super special grade, Wako Pure Chemical Industries
Sucrose	Special grade, Wako Pure Chemical Industries
Hydrofluoric acid	46–48 %, special grade, Wako Pure Chemical Industries
Calcium gluconate	Special grade, Wako Pure Chemical Industries
Amberlyst 70	Sulfonic acid cation exchange resin, Organo
JRC-Z5-90H	Proton-type MFI zeolite, Si/Al ratio = 45, Catalysis Society of Japan, denoted as H-MFI
JRC-Z-HM90	Proton-type MOR zeolite, Si/Al ratio = 45, Catalysis Society of Japan, denoted as H-MOR

Q-6	Amorphous silica, Fuji Silysia Chemical, denoted as SiO_2
Silica-alumina	Grade 135, Sigma-Aldrich, denoted as SiO_2-Al_2O_3
JRC-TIO-4(2)	Titania, Catalysis Society of Japan, denoted as TiO_2
Hydrochloric acid	35–37 %, special grade, Wako Pure Chemical Industries
Acetic acid	>99.7 %, special grade, Wako Pure Chemical Industries
Sodium acetate	Special grade, Wako Pure Chemical Industries
Sodium chloride	Special grade, Wako Pure Chemical Industries
Benzoic acid	Special grade, Wako Pure Chemical Industries
Cellohexaose	>95 %, Seikagaku Biobusiness
Cellopentaose	>95 %, Seikagaku Biobusiness
Cellotetraose	>97 %, Seikagaku Biobusiness
Cellotriose	>97 %, Seikagaku Biobusiness
D(+)-Cellobiose	Special grade, Kanto Chemical
D(+)-Glucose	Special grade, Kanto Chemical
D(+)-Mannose	Special grade, Wako Pure Chemical Industries
D(–)-Fructose	Special grade, Kanto Chemical
1,6-Anhydro-β-D-glucopyranose	99 %, Wako Pure Chemical Industries, denoted as levoglucosan
5-Hydroxymethylfurfural	99 %, Sigma-Aldrich, denoted as 5-HMF
Xylobiose	Biochemical grade, Wako Pure Chemical Industries
D(+)-Xylose	Special grade, Wako Pure Chemical Industries
D(–)-Arabinose	Special grade, Wako Pure Chemical Industries
Sodium sulfide	Special grade, Wako Pure Chemical Industries
Distilled water	Wako Pure Chemical Industries
Distilled water	For HPLC, Wako Pure Chemical Industries
Acetonitrile	For HPLC, Wako Pure Chemical Industries
Milli-Q water	Prepared by an ultrapure water production system (Sartorius, arium 611UF)
Lithium chloride	Special grade, Wako Pure Chemical Industries
N,*N*-Dimethylacetamide	Special grade, Wako Pure Chemical Industries, denoted as DMAc
Methanol	Special grade, Wako Pure Chemical Industries
Deuterium oxide	For NMR, Acros Organics
Deuterated methanol	For NMR, Acros Organics
Calcium carbonate	Special grade, Wako Pure Chemical Industries
Sodium hydrogen carbonate	Special grade, Wako Pure Chemical Industries
Sodium carbonate solution	For volumetric analysis, 0.05 M, Wako Pure Chemical Industries
Sodium hydroxide solution	For volumetric analysis, 0.05 M, Wako Pure Chemical Industries

Hydrochloric acid solution	For volumetric analysis, 0.05 M, Wako Pure Chemical Industries
Methyl orange	Special grade, Wako Pure Chemical Industries
Nitrogen gas	Alpha gas 2, Air Liquide Kogyo Gas
Oxygen gas	Alpha gas 2, Air Liquide Kogyo Gas
Argon gas	Alpha gas 2, Air Liquide Kogyo Gas

2.2.2 *Synthesis of Mesoporous Carbon CMK-3*

Mesoporous carbon CMK-3 was synthesized by following the literature [20]. Pluronic P123 (12 g) was completely dissolved in an HCl aqueous solution (1.6 M, 450 g) at 308 K, and subsequently TEOS (26 g) was added dropwise into the solution over *ca.* 3 min under vigorous stirring using a magnetic stir bar. The agitation was further continued for 15 min at 308 K. The sample was aged at 308 K for 24 h and then at 373 K for 24 h in an oven without stirring. During stirring and aging, the lid of vessel was kept closed. The resulting solid and liquid were separated by suction filtration using a Buchner funnel with filter paper (4A, hard type) and a filtering flask with ethanol as an antiform. The solid was washed with distilled water (1.5 L) and was dried at 373 K through the night in an oven. The resulting powder was calcined in an electric furnace (Yamato, FO610) at 833 K for 8 h, for which the ramping rate of temperature was 10 K min^{-1}. After the calcination, 6.7 g of white powder (mesoporous silica SBA-15) was obtained.

Synthesized SBA-15 (2.0 g) was dispersed in a sucrose aqueous solution [sucrose (2.5 g), H_2SO_4 (0.29 g), and distilled water (10 mL)], and the suspension was stirred at room temperature for 1 h to impregnate sucrose into the pores of SBA-15. After the filtration, the powder was dried at 373 K for 6 h and then at 433 K for 6 h. The powder was crashed on a mortar and was again dispersed in a sucrose solution [sucrose (1.6 g), H_2SO_4 (0.19 g), and distilled water (10 mL)]. After filtration and drying under the same conditions described above, the powder was heated to 1173 K by 2.4 K min^{-1}, and then the temperature was kept for 6 h in a horizontal quartz tube [inner diameter ø30 mm, temperature was controlled by an electric furnace (AZ ONE, TMF-300 N)] under N_2 flow (10 mL min^{-1}) to carbonize impregnated sucrose. The carbon/SBA-15 composite was dispersed in an HF aqueous solution (10 wt%, 100 g), and the suspension was stirred at room temperature for 4 h to dissolve the SBA-15 template. The suspension was separated by filtration using a Buchner funnel with filter paper (4A, hard type) and a filtering flask containing a calcium gluconate solution to quench HF. The resulting powder was washed with distilled water repeatedly and dried in an oven at 373 K overnight. Then, 1.2 g of black powder (mesoporous carbon CMK-3) was obtained.

2.2.3 Quantitative Analysis of OFGs on Carbon Materials

Carboxylic acids, lactones, and phenolic groups on carbon materials were quantified by the Boehm titration [22]. 0.5 g of carbon was dispersed in a base aqueous solution (50 mM, 20 mL, containing $NaHCO_3$, Na_2CO_3, or NaOH). The suspension was stirred at 600 rpm at 298 K for 24 h under Ar, and the liquid and solid were separated by filter paper (5A, quantitative) to remove carbon. Twice of a stoichiometric amount of HCl aqueous solution (50 mM) against base used was added to 5 mL of the filtrate. After sonication under 500 hPa of reduced pressure for 5 min to remove CO_2 dissolving in the solution, back titration was conducted using a 50 mM of NaOH aqueous solution with methyl orange as an indicator. Note that phenolphthalein is not suitable as an indicator since equilibrium of carbonate ion influences color change of phenolphthalein at high pH.

2.2.4 Analysis of Components in Bagasse Kraft Pulp

The weight ratio of cellulose, hemicellulose (xylan and arabinan), and lignin in bagasse kraft pulp was determined by following the established technique, so-called National Renewable Energy Laboratory (NREL) method [21]. 300 mg of bagasse kraft pulp was dispersed in 3 mL of H_2SO_4 aqueous solution (72 wt%), and the suspension was stirred at 303 K for 1 h. After adding 84 mL of distilled water to dilute H_2SO_4, the mixture was reacted at 394 K for 1 h in a hastelloy C22 high-pressure reactor (OM Lab-Tech, MMJ-100, 100 mL, Fig. 2.2). The solid and liquid phases were separated by filtration, and then $CaCO_3$ was added to the liquid phase to quench H_2SO_4 to be pH 7. The pH should be kept ≤7 to prevent sugars from their decomposition. The resulting solution was analyzed by high-performance liquid chromatography (HPLC, the conditions are shown in Sect. 2.2.6) to determine the amounts of glucose, xylose, and arabinose, corresponding to cellulose, xylan, and arabinan, respectively. The solid was washed with distilled water and dried in an oven at 378 K overnight and then was calcined in an electric furnace (Denken-Highdental, KDF-S90) at 848 K for 24 h under air. The amount of lignin was determined from weight decrease by the calcination.

2.2.5 Ball-Milling and Mix-Milling Pretreatment of Cellulose

Microcrystalline cellulose (10 g) was ball-milled in the presence of ZrO_2 balls (ø1.0 cm, 1 kg) in a ceramic pot (0.9 L) at 60 rpm for 96 h or in the presence of Al_2O_3 balls (ø1.5 cm, 2 kg) in a ceramic pot (3.6 L) at 60 rpm for 48 h. Mix-milling

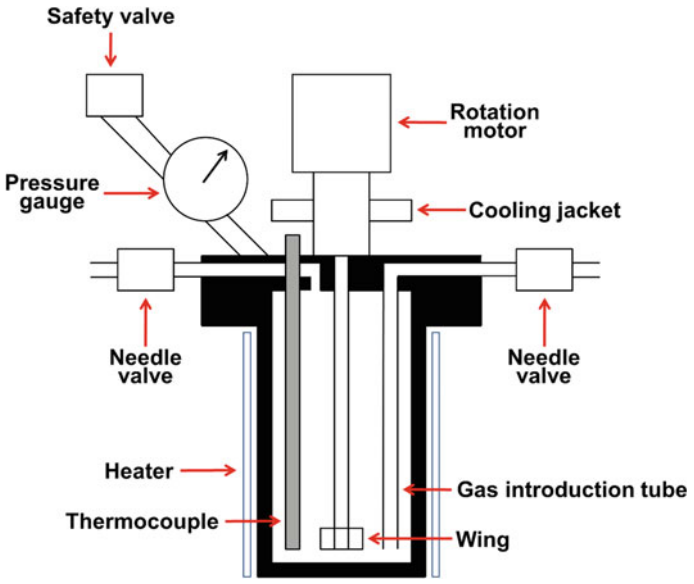

Fig. 2.2 Diagram of hastelloy C22 high-pressure reactor

of cellulose and solid catalyst was carried out in the same type of pot with the Al_2O_3 balls. Microcrystalline cellulose (10 g) and solid catalyst (1.54 g) (S/C ratio based on weight = 6.5) were added into the pot and were milled together at 60 rpm for 48 h. The amount of catalyst was reduced to 1.46 g for the mix-milling of cellobiose (S/C = 6.8).

Ball-milled samples were analyzed by XRD (Rigaku, MiniFlex, Cu Kα radiation), ^{13}C cross polarization/magic angle spinning NMR (^{13}C CP/MAS NMR, Bruker, MSL-300, 75 MHz, MAS frequency 8 kHz), laser diffraction (Nikkiso, Microtrac MT3300EXII, for estimation of secondary particle size), optical microscope (KEYENCE, VHX-5000), and scanning electron microscope (SEM, JEOL, JSM-6360LA). The viscometry was conducted at 303 K using an Ubbelohde viscometer (No. 0C) in 9 wt% LiCl/DMAc solvent [23]. The dissolution of cellulose in 9 wt% LiCl/DMAc was conducted by following the reported procedure [24]. 200 mg of cellulose sample was dispersed in 100 mL of Milli-Q water, and the suspension was stirred at room temperature overnight. The liquid phase was removed by centrifugation and decantation. The remaining solid was dispersed in 100 mL of methanol, and the suspension was stirred for 30 min at room temperature. After removing solvent by centrifugation and decantation, the solid was immersed in 50 mL of DMAc for 30 min at room temperature, and this procedure was repeated three times. Then, the resulting solid was dissolved in 9 wt% LiCl/DMAc. The prepared cellulose solution was used for the viscometry.

2.2.6 Catalytic Hydrolysis of Cellulosic Molecules

The hydrolysis of cellulose was conducted in the hastelloy C22 high-pressure reactor (Fig. 2.2). Ball-milled cellulose (324 mg), catalyst (50 mg), and distilled water (40 mL) were charged into the reactor. For the hydrolysis of mix-milled samples, 374 mg of the sample [containing cellulose (324 mg) and catalyst (50 mg)] and distilled water (40 mL) were used. The reactor was heated to 503 K in 18 min and then cooled to 323 K by blowing air for 22 min (named rapid heating-cooling condition, Fig. 2.3). The suspension was separated by centrifugation and decantation. The products in the aqueous phase were analyzed by HPLC [Shimadzu, LC10-AT*VP*, equipped with refractive index (RI) and ultraviolet (UV, 210 nm) detectors as well as a fraction collector] with a SUGAR SH1011 column (Shodex, ø8 × 300 mm, mobile phase: water at 0.5 mL min^{-1}, 323 K), a Rezex RPM-Monosaccharide Pb++ column (Phenomenex, ø7.8 × 300 mm, mobile phase: water at 0.6 mL min^{-1}, 343 K), and a TSKgel Amide-80 HR column [Tosoh, ø4.6 × 250 mm, mobile phase: acetonitrile/water (6/4, vol/vol) at 0.8 mL min^{-1}, 303 K]. An absolute calibration method was employed for calculation of product yields (Eq. 2.1). The conversion of cellulose was determined based on the weight difference of the solid part before and after reaction (Eq. 2.2).

$$(\text{Yield}/\%) = \frac{CF_{\text{HPLC}} \times A_{\text{HPLC}} \times V}{\frac{M_{\text{cellulose}}}{162.13}} \times \frac{n}{6} \times 100 \tag{2.1}$$

where CF_{HPLC} (unit: M $count^{-1}$) is calibration factor, A_{HPLC} (count) is peak area in HPLC chart, V (L) is volume of reaction solution, $M_{\text{cellulose}}$ (g) is mass of cellulose charged, and n is carbon number in a product.

$$(\text{Conversion}/\%) = \frac{M_{\text{residue}} - M_{\text{catalyst}}}{M_{\text{cellulose}}} \times 100 \tag{2.2}$$

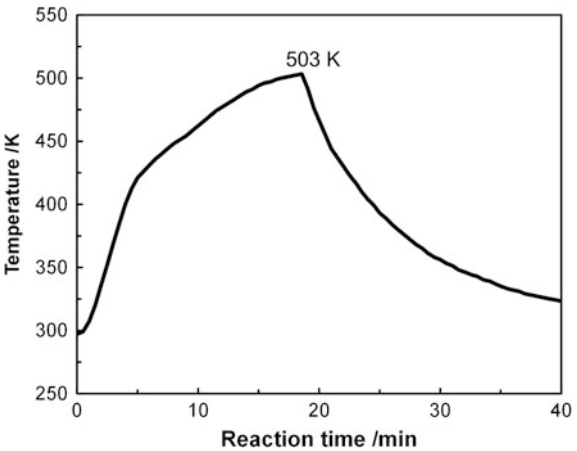

Fig. 2.3 Temperature profile of rapid heating-cooling condition

where $M_{residue}$ (unit: g) is mass of dried residue and $M_{catalyst}$ (g) is mass of catalyst charged.

The amount of organic carbons in reaction solution was quantified by measurement of total organic carbon (TOC, Shimadzu TOC-V_{CSN}) to determine conversion (Eq. 2.3) when catalyst was partially dissolved in water after the reaction (see Sect. 2.3.2).

$$(\text{Conversion}/\%) = \frac{CF_{TOC} \times A_{TOC}}{M_{cellulose} \times \frac{72.06}{162.13}} \times 100 \tag{2.3}$$

where CF_{TOC} (unit: gram-carbon count^{-1}) is calibration factor and A_{TOC} (count) is peak area in TOC measurement.

The products were identified by HPLC, liquid chromatography/mass spectroscopy [LC/MS, Thermo Fischer Scientific, LCQ Fleet, atmospheric pressure chemical ionization (APCI), the conditions were the same as those of HPLC], and ^{1}H NMR spectroscopy (JEOL, JNM-ECX400, 400 MHz).

The hydrolysis of mix-milled samples at a lower temperature (≤423 K) was carried out in a pressure-resistant glass tube (Ace Glass, 15 mL). 94 mg of mix-milled sample [containing cellulose (81 mg) and catalyst (13 mg)] and distilled water (10 mL) were charged into the tube. The tube was immersed in an oil bath at a certain temperature for a designated length of time. The product analysis was performed using the same procedure described above.

The hydrolysis of cellobiose was conducted in the hastelloy C22 high-pressure reactor. Cellobiose (342 mg), catalyst (50 mg), and distilled water (40 mL) were charged into the reactor. The temperature was raised to 463 K in 11 min, and then the reactor was rapidly cooled to 323 K by blowing air. The product yield and conversion were determined by HPLC (vide supra).

2.2.7 *Reuse Test of Mix-Milled Cellulose*

Microcrystalline cellulose (10 g) and K26 (1.54 g) were ball-milled together in the presence of the Al_2O_3 balls (ø1.5 cm, 2 kg) in the ceramic pot (3.6 L) at 60 rpm for 48 h. The recovered sample and 0.012 wt% HCl aqueous solution (40 mL) were charged into the hastelloy C22 high-pressure reactor (Fig. 2.2). The temperature was first raised to 473 K and was maintained for 2 min. Then, the reactor was cooled down to 423 K by blowing air and the mixture was further reacted for 60 min at the temperature. After cooling down to room temperature, the solid and liquid phases were separated by centrifugation and decantation. The solid phase was washed with distilled water repeatedly to extract physisorbed products, for which total volume of water used was *ca.* 160 mL. The resulting solid was dried under vacuum overnight at 353 K. The liquid phase and washing solvent were mixed and then analyzed by HPLC (vide supra). In the next run, the dried solid was

mix-milled with fresh cellulose, the amount of which was the same as that of converted cellulose in the previous run. The experimental schemes are drawn in Sect. 2.3.2.

2.3 Results and Discussion

2.3.1 Screening of Carbon Catalysts for Hydrolysis of Cellulose

First, catalytic activity of various carbon materials has been investigated for the hydrolysis of individually ball-milled cellulose in water under the rapid heating–cooling condition at 503 K (Fig. 2.3), and Table 2.1 summarizes the reaction results. Among the carbon materials tested, alkali-activated carbon K26 was the most active catalyst and converted 60 % of cellulose (entry 2). The main product was glucose with 36 % yield, which was clearly higher than that in a control experiment without catalysts (4.6 %, entry 1). The other identified products were water-soluble oligosaccharides (2.5 %, DP = mainly 2–6), fructose (2.7 %), mannose (2.6 %), levoglucosan (2.1 %), and 5-HMF (3.4 %). Unidentified water-soluble compounds (16 %) were also formed, the yield of which was calculated from carbon balance. In repeated reactions, K26 maintained its catalytic performance at least four times.

Table 2.1 Hydrolysis of individually ball-milled cellulose by carbon catalysts

Entry	Catalyst	Conv./%	Yield based on carbon/%						
			Glucan		By-product				
			Glc[a]	Olg[b]	Frc[c]	Man[d]	Lev[e]	HMF[f]	Others[g]
1	None	28	4.6	15	0.5	0.6	0.2	1.8	5.3
2	K26	60	36	2.5	2.7	2.6	2.1	3.4	11
3	K20	59	35	1.7	1.9	1.3	2.7	2.9	14
4	MSP20	50	26	6.3	1.7	1.6	1.6	2.1	11
5	BA50	57	17	20	1.0	1.0	0.9	3.5	14
6	CMK-3	52	12	25	0.9	0.8	0.7	2.5	10
7	SX	38	8.1	20	0.6	0.9	0.4	1.4	6.6
8	BP2000	37	6.4	12	0.5	0.5	0.3	1.8	16
9	XC72	35	5.8	19	0.6	0.9	0.2	1.9	6.6

Conditions individually ball-milled cellulose (0.9 L pot) 324 mg; catalyst (not milled) 50 mg; distilled water 40 mL; 503 K; rapid heating-cooling condition (Fig. 2.3)

[a]Glucose

[b]Water-soluble oligosaccharides (DP = mainly 2–6)

[c]Fructose

[d]Mannose

[e]Levoglucosan

[f]5-HMF

[g](Conversion) – (Total yield of identified products)

Alkali-activated carbon K20 showed similar catalytic activity to K26, and gave 59 % conversion of cellulose and 35 % yield of glucose (entry 3). Another alkali-activated carbon MSP20, steam-activated carbon BA50, and mesoporous carbon CMK-3 were less active than K26 and K20 (entries 4–6). The other carbons, steam-activated carbon SX, carbon black BP2000, and carbon black XC72 were almost inactive (entries 7–9). These results show that catalytic activity of carbon materials strongly depends on their chemical and/or physical properties, derived from precursors and synthetic methods. Consequently, K26, which can be synthesized in a bulk scale in industry, showed a significantly higher catalytic activity than CMK-3, and thus K26 was mainly used for further study.

Next, the amounts of carboxylic acids, lactones, and phenolic groups as OFGs on carbons were quantified by the Boehm titration [22] (Table 2.2). The highly active catalysts such as K26 and K20 contain a large amount of OFGs (entries 10

Table 2.2 Amount of OFGs on carbon materials

Entry	Carbon	OFGs/μmol g^{-1}				Conv.[a]/%	Glc[a,b]/%
		Carboxylic acids	Lactones	Phenolic groups	Total		
10	K26	270	310	310	880	60	36
11	K20	420	270	320	1010	59	35
12	MSP20	65	110	280	450	50	26
13	CMK-3	140	97	180	410	52	12
14	SX	80	49	34	160	38	8.1
15	BP2000	61	12	88	160	37	6.4
16	XC72	26	49	0	75	35	5.8

Determined by the Boehm titration [22]
[a]Reaction conditions: individually ball-milled cellulose (0.9 L pot) 324 mg; catalyst (not milled) 50 mg; distilled water 40 mL; 503 K; rapid heating-cooling condition (Fig. 2.3). The detailed results are summarized in Table 2.1
[b]Glucose yield

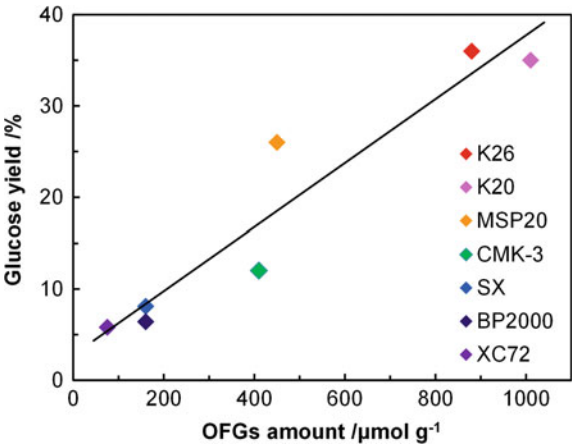

Fig. 2.4 Effect of OFGs amount on catalytic activity of carbons

and 11), and less active catalysts do lower amounts (entries 12–16). The total amount of OFGs on carbons positively correlates with catalytic activity for glucose production from cellulose (Fig. 2.4), indicating that weakly acidic OFGs may be active sites. However, this trend would also include the influence of physical properties of each carbon material, and the detailed functions of OFGs are discussed in Chap. 3. It is notable that K26 does not contain sulfonic groups since the sulfur content is less than 0.01 %. This amount of sulfur corresponds to only $<10^{-5}$ % in the whole reaction mixture and does not catalyze the reaction at all. In fact, the hydrolysis in the presence of even 10^{-4} % H_2SO_4 provided 4.3 % yield of glucose (Table 2.3, entry 17) as low as the yield of blank experiment (4.6 %, entry 1). The author further conducted control experiments to evaluate acidity of active sites. K26 was treated in AcOH/AcONa (pH 4.0), NaCl (pH 7.0), $NaHCO_3$ (pH 8.3), and NaOH (pH 12.6) to neutralize corresponding acidic sites on K26 and the treated carbons were subjected to the hydrolysis of individually ball-milled cellulose (Fig. 2.5). The acetate buffer treatment did not influence the catalytic activity of K26, indicating that no strong acid worked as a predominant active site. Similarly, K26 has resisted an actual salt NaCl; K26 possibly maintains its catalytic activity even in the presence of salts. The $NaHCO_3$-treated K26 still produced glucose in 13 % yield, but exposure to NaOH completely deactivated K26 due to neutralization

Table 2.3 Control experiments on hydrolysis of individually ball-milled cellulose

Entry	Solvent	Conv./ %	Yield based on carbon/%						
			Glucan		By-product				
			Glc[a]	Olg[b]	Frc[c]	Man[d]	Lev[e]	HMF[f]	Others[g]
1	Distilled water	28	4.6	15	0.5	0.6	0.2	1.8	5.3
17	10 μM H_2SO_4[h]	29	4.3	17	0.8	0.8	0.2	1.9	3.9
18	50 μM AcOH[i]	26	3.8	17	0.8	0.8	0.2	2.0	1.9
19	Filtrate of used K26[j]	22	3.1	13	0.5	0.6	0.1	1.4	2.9
20	Filtrate of used K26 and cellulose[k]	39	n.d.[l]	n.d.[l]	n.d.[l]	n.d.[l]	n.d.[l]	n.d.[l]	n.d.[l]

Conditions individually ball-milled cellulose (0.9 L pot) 324 mg; solvent *ca.* 40 mL; 503 K; rapid heating-cooling condition (Fig. 2.3)

[a]Glucose

[b]Water-soluble oligosaccharides (DP = mainly 2–6)

[c]Fructose

[d]Mannose

[e]Levoglucosan

[f]5-HMF

[g](Conversion) – (Total yield of identified products)

[h]pH = 4.7

[i]pH = 4.6

[j]The filtrate of K26 aqueous mixture subjected to the rapid heating–cooling condition (Fig. 2.3) was used as a solvent instead of distilled water

[k]The filtrate of the mixture of the cellulose hydrolysis by K26 (Table 2.1, entry 2) was used as a solvent instead of distilled water

[l]The values were unable to be determined because products formed from cellulose in the primary reaction (Table 2.1, entry 2) were contained, and they remained as themselves and/or underwent the degradation during this reaction

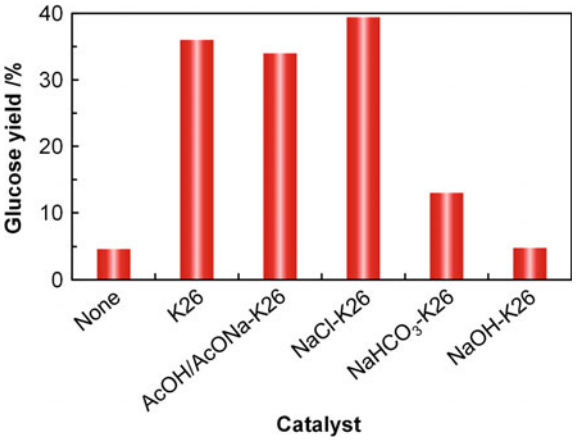

Fig. 2.5 Hydrolysis of individually ball-milled cellulose by base-treated K26. Conditions: individually ball-milled cellulose (0.9 L pot) 324 mg; catalyst 50 mg; distilled water 40 mL; 503 K; rapid heating-cooling condition (see Fig. 2.3)

of all acid sites. Hence, the hydrolytic activity of K26 may be ascribed to weakly acidic groups such as carboxylic acids and phenolic groups. These results also suggest that weak acids are advantageous over strong acids owing to the resistance to salts derived from raw biomass since strong acids easily undergo ion exchange to be deactivated even in an acetate buffer [18, 19].

The author investigated whether the most active catalyst K26 worked as a *solid* catalyst in the hydrolysis of cellulose. The dispersion of K26 into distilled water caused the drop of pH to 4.9 due to weakly acidic OFGs. The same phenomenon is also observed when dispersing solid acids such as zeolites in water [25–27]. After filtration with a polytetrafluoroethylene (PTFE) membrane to remove K26, the pH value returned to almost neutral (5.8). This result confirmed that the pH decrease was not caused by leaching of soluble acidic species from K26. The acidic solutions with the same pH value as that of the K26 suspension, i.e., 10 μM H_2SO_4 (pH 4.7) and 50 μM AcOH (pH 4.6), were not active for the hydrolysis of cellulose at all (Table 2.3, entries 17 and 18). As it is known that the hydrolysis by H_3O^+ is negligible at pH higher than 4 [28], the promotion of the hydrolysis by K26 is not ascribed to the buffering effect releasing H_3O^+ in the suspended state. In addition to these evidences, the filtrates of the K26 suspension and K26-cellulose one, which were subjected to the reaction conditions at 503 K (Fig. 2.3), were less active (entries 19 and 20) than *solid* K26 itself (entry 2). Although the filtrate in entry 20 possibly contained soluble acidic by-products formed in the primary reaction of cellulose, the catalytic effects of the acidic species were limited in the hydrolysis of cellulose; they enhanced only 11 % of cellulose conversion from the blank reaction (entry 1). Hence, K26 should hydrolyze cellulose as a *solid* catalyst. The author also confirmed whether cellulose underwent hydrolysis as a *solid* substrate. The DP of ball-milled cellulose was 640, determined by viscometry (see Sect. 2.3.3), the value of which was high enough to be insoluble in water. The ball-milled cellulose did not contain a considerable amount of soluble oligomers (only 0.3 %), verified by the extraction with 40 mL of boiling water. Meanwhile, it has been reported that

cellulose slightly dissolves in water at ambient temperature (*ca.* 2×10^{-3} wt%) [29] and complete dissolution of cellulose in water requires high temperatures as well as extremely high pressures (e.g., 603 K, 345 MPa) [30]. These reports motivated the author to estimate the influence of cellulose solubility on the hydrolysis at 503 K. If the slightly soluble portion of cellulose was responsible for the reaction, the hydrolysis rate should depend on the saturated solubility of cellulose, giving a constant concentration of dissolved cellulose. In contrast to the hypothesis, the conversion rate increased linearly with increasing amount of solid cellulose (Table 2.4 and Fig. 2.6). Although the possibility of soluble active species or partial dissolution of the substrate is not completely excluded, these results show that *solid* cellulose undergoes the hydrolysis catalyzed mainly by *solid* K26. Hence, both carbon and cellulose behave as solids in the hydrolysis, namely solid–solid reaction.

Table 2.4 Effect of cellulose amount on hydrolysis by K26

Entry	Amount of ball-milled cellulose/g L^{-1}	Conv./%	Conv. rate[a]/g L^{-1} h^{-1}	Yield based on carbon/%						
				Glucan		By-product				
				Glc[b]	Olg[c]	Frc[d]	Man[e]	Lev[f]	HMF[g]	Others[h]
21	8.1	72	8.7	40	1.4	2.1	1.8	2.8	5.4	19
22	16	66	16	40	1.5	1.7	1.3	2.5	6.3	13
23	24	66	24	39	1.7	1.4	1.2	2.6	7.0	13
24	40	58	35	38	2.1	1.3	1.2	2.2	6.7	7.2

Conditions K26 50 mg; distilled water 40 mL; 508 K; rapid heating-cooling condition (Fig. 2.3). Cellulose was ball milled without catalyst in a 0.9 L pot

[a]Conversion rate of cellulose based on the total reaction time (40 min, see Fig. 2.3)

[b]Glucose

[c]Water-soluble oligosaccharides (DP = mainly 2–6)

[d]Fructose

[e]Mannose

[f]Levoglucosan

[g]5-HMF

[h](Conversion) – (Total yield of identified products)

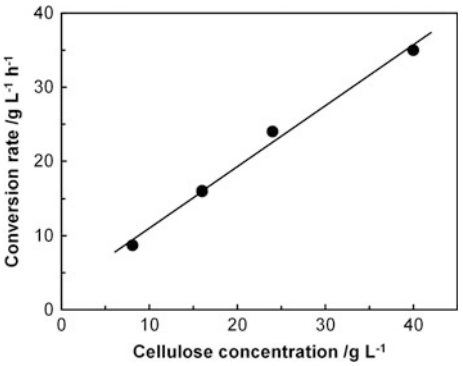

Fig. 2.6 Effect of cellulose amount on conversion rate

In solid–solid reactions, a collision between a solid substrate and a solid catalyst is limited, hampering reaction proceeding. In other words, solid catalysts would unsatisfactorily show their catalytic performance during reactions because of loose contact with a substrate.

2.3.2 *High-Yielding Production of Glucose from Cellulose*

In the previous section, K26 has provided glucose in 36 % yield from individually ball-milled cellulose (Table 2.1, entry 2), but the yield needs to be improved for practical use. The hydrolysis of cellulose by carbon catalyst takes place at their interface, namely solid–solid reaction; loose contact between a solid substrate and a solid catalyst is an obstacle. The author therefore employed a new pretreatment method named *mix-milling*, ball-milling cellulose and catalyst together, to make tight contact (Fig. 2.7).

The various solid materials including carbons and typical solid acids were tested for the hydrolysis of cellulose at 453 K for 20 min after the mix-milling pretreatment. In control experiments employing individually ball-milled cellulose as a substrate, the hydrolysis in the presence/absence of solid catalysts provided poor reaction results (7.9–15 % yields of glucans, Table 2.5, entries 25–34). The results of the hydrolysis of mix-milled cellulose are also shown in Table 2.5 (entries 35–43). K26 produced water-soluble glucans in 90 % yield [glucose (20 %) and oligosaccharides (70 %)] with 97 % selectivity (entry 35). The other products were fructose (0.6 %), mannose (0.7 %), levoglucosan (0.7 %), 5-HMF (1.0 %), and unidentified compounds (<1 %). The solid residue containing K26 was easily separated from the product cocktail by filtration after the reaction (Fig. 2.8). The mix-milling pretreatment also enhanced the yields of glucans when employing the other carbon materials, BA50 (34 %, entry 36) and SX (22 %, entry 37), compared to the individual milling (entries 27 and 28). However, these carbons were less active than K26 due to lower amounts of weakly acidic groups as described in Sect. 2.3.1. A sulfonic acid cation exchange resin Amberlyst 70 afforded remarkably high glucose yield (82 %, entry 38). After mix-milling of cellulose with Amberlyst 70, >99 wt% of the sample dissolved as various kinds of oligosaccharides [31]

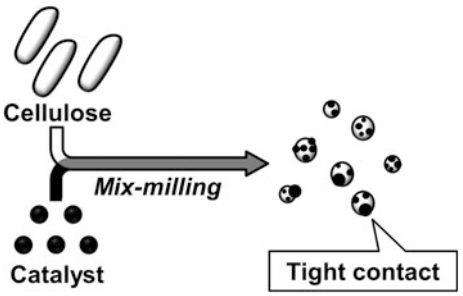

Fig. 2.7 Schematic of mix-milling pretreatment

Table 2.5 Effect of pretreatment on hydrolysis of cellulose by various solid catalysts

Entry	Catalyst	Pretreatment	Conv./ %	Yield based on carbon/%						
				Glucan		By-product				
				Glc[a]	Olg[b]	Frc[c]	Man[d]	Lev[e]	HMF[f]	Others[g]
25	None	Individual[k]	12	1.3	6.6	0.2	0.2	<0.1	0.2	3.4
26	K26	Individual[l]	18	2.9	10	0.5	0.4	0.1	<0.1	3.7
27	BA50	Individual[k]	20	2.4	8.6	0.2	0.3	<0.1	<0.1	8.0
28	SX	Individual[k]	16	2.3	8.0	0.3	0.3	<0.1	<0.1	4.8
29	Amberlyst 70	Individual[k]	18	6.3	8.2	0.2	0.8	0.2	0.3	2.4
30	H-MFI	Individual[k]	16	3.2	9.1	0.3	0.2	0.1	0.1	3.3
31	H-MOR	Individual[k]	17	3.8	9.6	0.3	0.3	0.1	0.2	3.0
32	SiO_2-Al_2O_3	Individual[k]	7.0	0.9	5.4	0.2	0.2	<0.1	0.2	0.1
33	SiO_2	Individual[k]	12	2.1	8.3	0.3	0.4	<0.1	0.2	1.1
34	TiO_2	Individual[k]	14	2.3	9.7	0.4	0.4	0.1	0.3	0.2
35	K26	Mix[m]	93	20	70	0.6	0.7	0.7	1.0	<1[n]
36	BA50	Mix[m]	35	6.7	27	0.7	0.7	0.2	0.2	0.2
37	SX	Mix[m]	24	4.2	18	0.8	0.5	0.1	0.3	0.1
38	Amberlyst 70	Mix[m]	>99	82	1.9	0.5	1.4	2.6	2.8	8.8
39	H-MFI	Mix[m]	19	4.0	11	0.4	0.3	0.1	0.2	3.2
40	H-MOR	Mix[m]	21	4.9	11	0.4	0.3	0.2	0.5	4.0
41	SiO_2-Al_2O_3	Mix[m]	6.8	0.9	4.8	0.2	0.2	<0.1	0.2	0.5
42	SiO_2	Mix[m]	16	3.4	11	0.3	0.3	0.1	0.3	0.1
43	TiO_2	Mix[m]	13	1.6	7.1	0.5	0.3	<0.1	0.4	2.6
44	K26, HCl[i]	Mix[m]	98	88	2.7	1.5	1.5	3.0	1.7	<1[n]
45	K26, H_2SO_4[j]	Mix[m]	95	69	8.6	0.7	1.3	2.2	1.8	11
46	HCl[i]	Individual[j]	39	27	3.9	1.8	1.8	1.0	1.6	1.8
47	K26, HCl[i]	Individual[l]	40	30	4.3	1.3	1.3	1.1	0.7	0.7
48[h]	K26	Mix[m]	97	72	2.8	1.4	1.5	1.4	4.9	13

Conditions cellulose 324 mg; catalyst 50 mg; distilled water 40 mL; 453 K; 20 min. For hydrolysis of mix-milled cellulose, 374 mg of sample (containing cellulose 324 mg and catalyst 50 mg) was used

[a]Glucose

[b]Water-soluble oligosaccharides (DP = mainly 2–6)

[c]Fructose

[d]Mannose

[e]Levoglucosan

[f]5-HMF

[g](Conversion) – (Total yield of identified products)

[h]Conditions: mix-milled cellulose 94 mg (containing cellulose 81 mg and K26 13 mg); distilled water 10 mL; 418 K; 24 h

[i]Hydrolysis was conducted in a 0.012 wt% HCl solution (pH 2.5)

[j]Hydrolysis was conducted in a 0.018 wt% H_2SO_4 solution (pH 2.5)

[k]Cellulose was ball-milled without catalyst in a 3.6 L pot. Catalyst was not ball-milled

[l]Cellulose and K26 were separately ball-milled

[m]Cellulose and catalyst were ball-milled together, namely mix-milling

[n]The total yield of others was not correctly determined because of high conversion

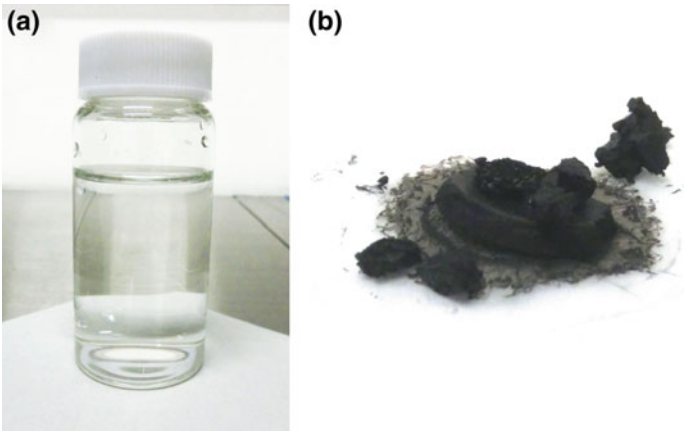

Fig. 2.8 Pictures of **a** product cocktail and **b** solid residue after hydrolysis of mix-milled cellulose containing K26. The solid and liquid phases were separated with a PTFE membrane (0.1 μm mesh)

in 40 mL of distilled water at room temperature, indicating that mechanocatalytic hydrolysis of cellulose [31–33] happened during the milling process in the presence of strong acidic species derived from the resin. The water-soluble oligosaccharides are hydrolyzed more easily than robust cellulose, resulting in the high-yielding production of glucose. However, the reaction solution was completely homogeneous (Fig. 2.9), and Amberlyst 70 was unable to be recovered by centrifugation at

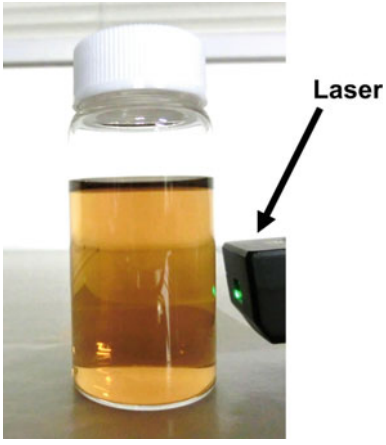

Fig. 2.9 Reaction mixture after hydrolysis of mix-milled cellulose containing Amberlyst 70. No solids were obtained after the reaction. The solution was irradiated with a green laser from right side of the bottle, but the Tyndall effect was hardly observed, showing that the solution was homogeneous and did not contain colloids

4600*g* (4.5×10^4 m s^{-2}) or filtration using a PTFE membrane (0.1 μm mesh), which was in sharp contrast to the behavior of K26 is shown in Fig. 2.8. The other materials (H-MFI, H-MOR, SiO_2-Al_2O_3, SiO_2, and TiO_2) were almost inactive even though employing the mix-milling pretreatment (entries 39–43). Moreover, these materials except TiO_2 partially dissolved in water during the reaction (Fig. 2.10).

K26 was the most active catalyst in the hydrolysis of mix-milled cellulose among the solid materials tested except for Amberlyst 70. There are two possibilities for this: crystalline structure of cellulose contained in each mix-milled sample (see Sect. 1.2.2) as well as activity of each catalyst. To evaluate the influence of crystallinity of cellulose on the hydrolysis, all the mix-milled samples were characterized by XRD. The XRD patterns of all mix-milled samples (Fig. 2.11) were the same as that of amorphous cellulose (shown as individually milled cellulose in figure), and no peak derived from crystalline cellulose was observed. The mix-milling pretreatment similarly degraded crystalline cellulose to amorphous one regardless of the presence of various solids. Hence, the difference in reaction results is not ascribed to the nature of cellulose but to activity of each catalyst.

The mix-milled cellulose containing K26 gave glucose and water-soluble oligosaccharides in 20 and 70 % yields, respectively, as already shown above (Table 2.5, entry 35). In order to further improve glucose yield by accelerating depolymerization of oligosaccharides to glucose, a 0.012 % HCl aqueous solution

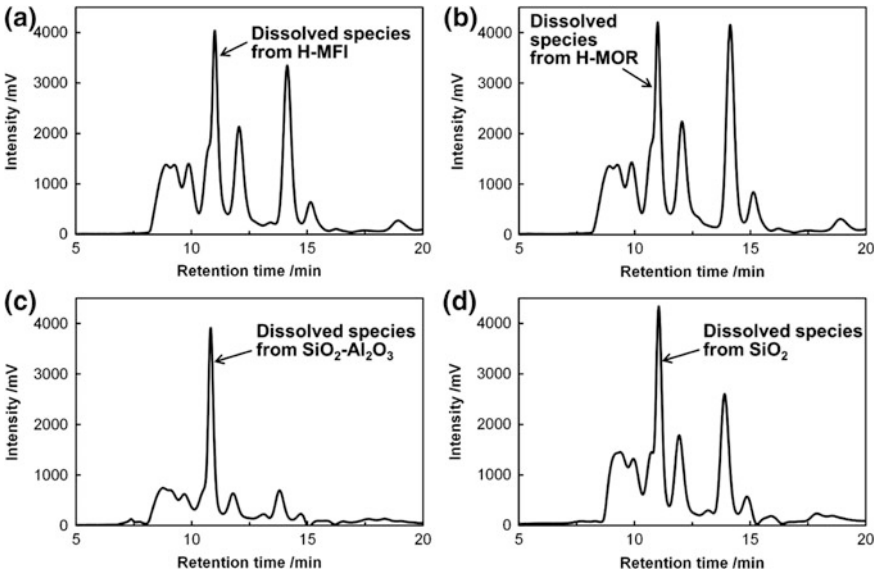

Fig. 2.10 HPLC charts for hydrolysis of mix-milled cellulose containing **a** H-MFI, **b** H-MOR, **c** SiO_2-Al_2O_3, and **d** SiO_2. Column: Rezex RPM-Monosaccharide Pb++. Detector: RI. Reaction conditions: mix-milled cellulose 374 mg (containing cellulose 324 mg and catalyst 50 mg); distilled water 40 mL; 453 K; 20 min

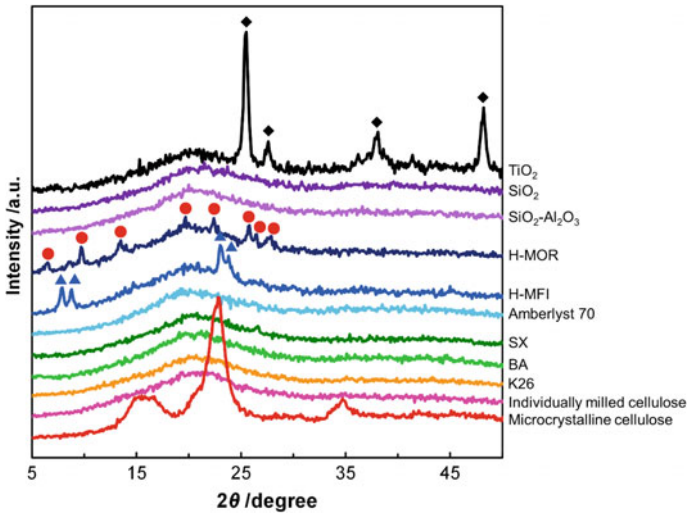

Fig. 2.11 XRD patterns of mix-milled samples containing cellulose and solid catalysts. The peaks marked with *black diamonds*, *red circles*, and *blue triangles* are from TiO_2, H-MOR, and H-MFI, respectively

(pH 2.5) was utilized as a solvent instead of water. This trace amount of HCl neither corrodes common stainless steel reactors nor has a negative economic impact because of very low concentration and low price [0.07–0.1 USD kg^{-1} as concentrated HCl in 2014 according to International Chemical Information Service (ICIS)] [34, 35]. Figure 2.12 shows the time course of the hydrolysis of mix-milled cellulose containing K26 conducted in the trace HCl aqueous solution at 453 K. In the initial stage of the reaction (≤2 min), water-soluble oligosaccharides were predominantly formed. Subsequently, the yield of glucose increased up to 88 % at 20 min and the selectivity of glucose based on cellulose conversion (98 %) was 90 % (Table 2.5, entry 44). This is the best result achieved in this work and one of the highest yields of glucose ever reported in any methods. After 20 min, the yield of glucose decreased because of the decomposition. Although an H_2SO_4 aqueous solution (0.018 wt%, pH 2.5) was advantageous over HCl due to its lower price (0.05 USD kg^{-1} in 2009 according to Nexant [36]) and less corrosive property, H_2SO_4 provided by 19 % lower yield of glucose than HCl at the same pH (entry 45). This result was possibly caused by the negative effect of SO_4^{2-} species on the hydrolysis reaction (Table 2.6); SO_4^{2-} species may prevent the activation of glycosidic bonds by forming a chelate. Therefore, the 0.012 wt% of HCl aqueous solution was employed as a reaction solvent in the following study. Note that such high-yielding production of glucose was unable to be achieved without the mix-milling pretreatment. Two types of control experiments were conducted as follows: the hydrolysis of individually ball-milled cellulose in the trace HCl (entry 46) and that of individually ball-milled cellulose by individually ball-milled K26 in

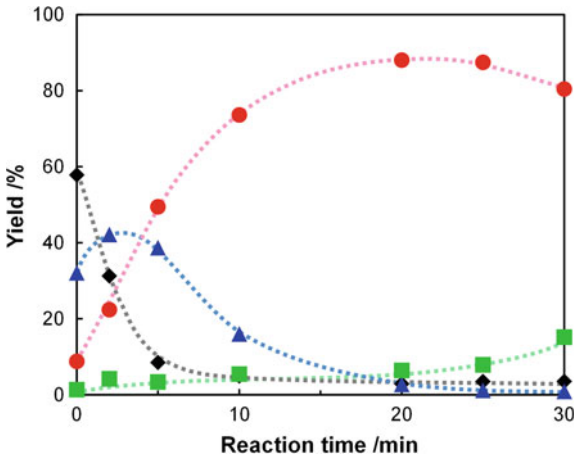

Fig. 2.12 Time course of hydrolysis of mix-milled cellulose containing K26 in 0.012 wt% HCl solution at 453 K. Conditions: mix-milled cellulose 374 mg (cellulose 324 mg and K26 50 mg); 0.012 wt% HCl solution 40 mL. Legends: *black diamonds* cellulose; *red circles* glucose; *blue triangles* oligosaccharides; and *green squares* by-products. In figure, the data sets at 0 min are for the hydrolysis under rapid heating–cooling condition (see Fig. 2.3). *Dashed lines* are simply smooth lines for connecting experimental data

Table 2.6 Inhibitory effect of salts on hydrolysis of cellulose

Entry	Salt	Conv./%	Yield based on carbon/%						
			Glucan		By-product				
			Glc[a]	Olg[b]	Frc[c]	Man[d]	Lev[e]	HMF[f]	Others[g]
1	None	28	4.6	15	0.5	0.6	0.2	1.8	4.8
49	3.2 mM NaCl	15	1.7	5.6	0.4	0.7	0.1	1.0	1.2
50	1.6 mM Na_2SO_4	6.7	0.3	2.3	0.1	0.1	0.4	0.2	3.4

Conditions individually ball-milled cellulose 324 mg (0.9 L pot); salt solution 40 mL; 503 K; rapid heating–cooling condition (Fig. 2.3)
[a]Glucose
[b]Water-soluble oligosaccharides (DP = mainly 2–6)
[c]Fructose
[d]Mannose
[e]Levoglucosan
[f]5-HMF
[g](Conversion) – (Total yield of identified products)

the HCl aqueous solution (entry 47). These control reactions yielded glucose in 20 and 30 %, which were significantly lower than the highest yield (88 %, entry 44). Similarly, the values of cellulose conversion were only 39 and 40 % in these control reactions. Neither the trace HCl nor individually ball-milled K26 accelerated the hydrolysis of cellulose in good performance due to low H^+ concentration and loose contact with the substrate. The mix-milling pretreatment is clearly essential for high-yielding production of glucose from cellulose.

The durability of K26 in this system was evaluated as the following procedure (see Sect. 2.2.7 as well as the schemes in Figs. 2.13 and 2.14): microcrystalline cellulose and K26 were milled together (i.e., mix-milling pretreatment); the hydrolysis of mix-milled cellulose in the 0.012 wt% HCl aqueous solution was operated at high loadings of the solid (cellulose 200 g L^{-1} and K26 31 g L^{-1}); the solid residue containing used K26 and unreacted cellulose was recovered, washed with distilled water repeatedly, and dried under vacuum; the resulting solid was ball-milled with fresh microcrystalline cellulose, the amount of which was equivalent to that of consumed cellulose in the previous run to maintain an S/C ratio; and the next run was conducted. This cycle was repeated several times. Figure 2.13 represents the results of reuse experiments at high cellulose conversion (88–91 %), and glucose was obtained in 71, 72, 70, and 67 % yields. Although these values were lower than the best glucose yield in this work (88 % at 8.1 g L^{-1}, Table 2.5, entry 44) probably due to the significantly high loadings of the solid, the high concentration of glucose clears the practical demand (10 wt%) to avoid energy-consuming condensation process of reaction product. Another type of reuse experiments at lower cellulose conversion was also performed (Fig. 2.14), in which yields of products and cellulose conversion gradually increased. This trend is reasonable since the residual solid cellulose has partially undergone hydrolysis to

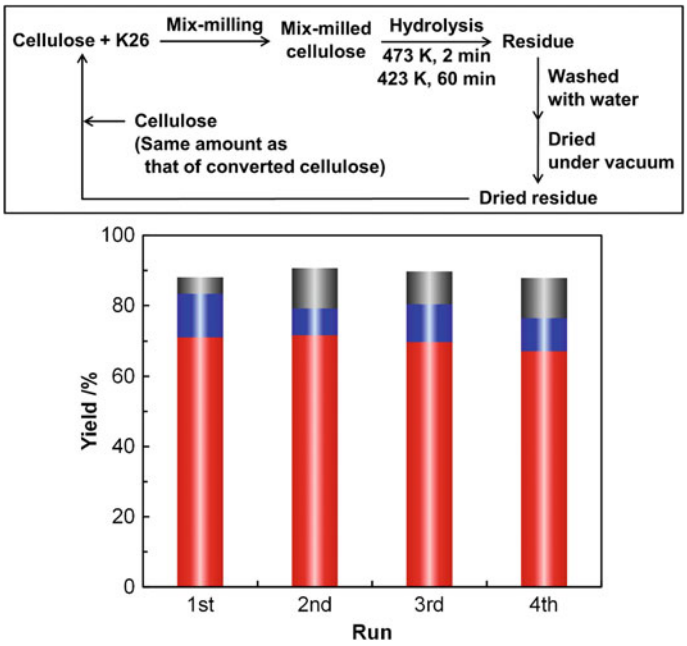

Fig. 2.13 Reuse experiments of mix-milled K26 for hydrolysis of cellulose (200 g L^{-1}) in 0.012 wt% HCl solution with high conversion. Legends: *red bar* glucose; *blue bar* oligosaccharides; and *gray bar* by-products

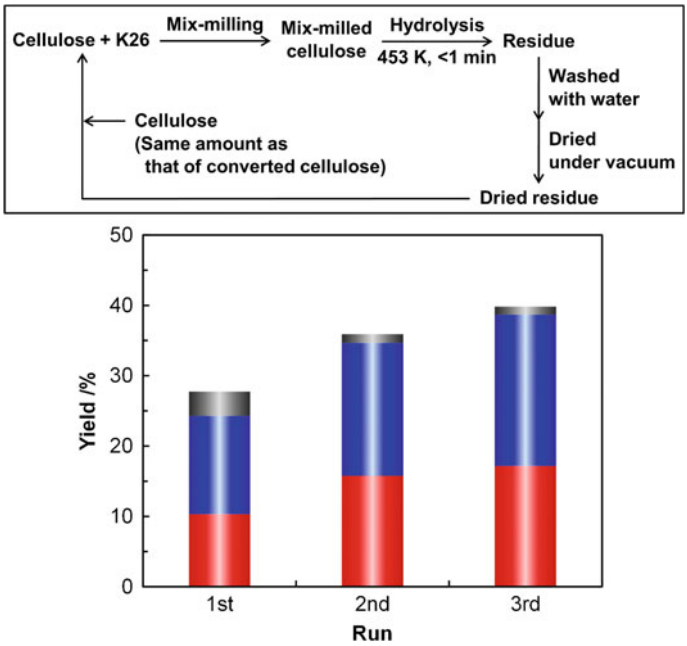

Fig. 2.14 Reuse experiments of mix-milled K26 for hydrolysis of cellulose (200 g L^{-1}) in 0.012 wt% HCl solution with low conversion. Legends: *red bar* glucose; *blue bar* oligosaccharides; and *gray bar* by-products

decrease DP in the previous run, which make this remaining part more reactive in the subsequent runs. These results in both high and low conversions show that the degradation rate of cellulose does not decrease during the repeated reactions. Hence, K26 is fairly stable during the mix-milling pretreatment as well as the hydrolysis in the presence of trace HCl and high concentrations of products.

Toward practical applications, the author demonstrated the saccharification of bagasse kraft pulp as a real biomass substrate by the inexpensive and commercially available steam-activated carbon BA50, which showed catalytic activity in cellulose conversion (Table 2.5, entry 36). The pulp contained cellulose (59 wt%), hemicellulose [xylan (25 wt%) and arabinan (2 wt%)], and lignin (9 wt%). At first, one-pot hydrolysis ofboth cellulose and hemicellulose in the bagasse kraft pulp was performed in the 0.012 wt% HCl solution for 2 min at various temperatures (Fig. 2.15) after mix-milling pretreatment. The yields of xylose andarabinose based on the amount of hemicellulose in the pulp were 89 and 5.2 % at 473 K, respectively. In this case, glucose yield based on the amount of cellulose in the pulp was only 32 %. The glucose yield increased up to 72 % with increasing the reaction temperature to 493 K, whereas the xylose yield decreased to 45 % due to the degradation. One-pot high-yielding production of both hexoses and pentoses is

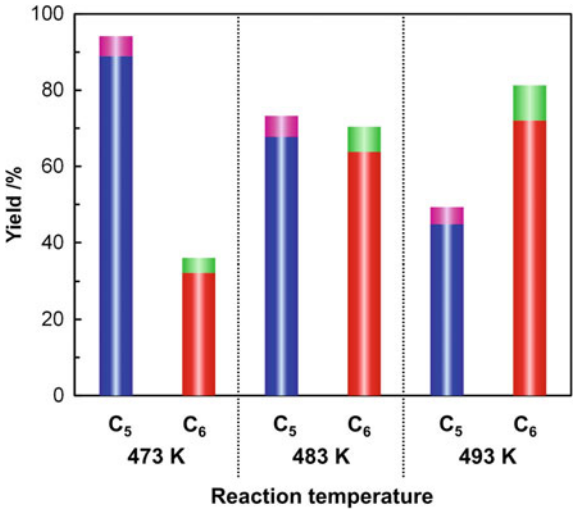

Fig. 2.15 One-pot hydrolysis of both cellulose/hemicellulose in bagasse kraft pulp at various temperatures for 2 min. Conditions: mix-milled bagasse craft pulp 374 mg (pulp 324 mg and BA50 50 mg); 0.012 wt% HCl solution 40 mL. Legends: *blue bar* xylose; *pink bar* arabinose; *red bar* glucose; and *green bar* fructose and mannose

difficult. Xylan is known as a more reactive substrate than cellulose due to the lack of an OH group at C6, which would make cellulose more chemically stable by forming hydrogen bonds (Fig. 2.16) [37]. In fact,xylobiose (the smallest model of xylan) was five times more reactive for the hydrolysis than cellobiose (that of cellulose) at 443 K for 10 min (Fig. 2.17). Taking account of the different reactivity of hemicellulose andcellulose, a cascade reaction was applied; the hydrolysis at 453 K for 1 min and subsequently at 483 K for 2 min (see the scheme in Fig. 2.18). In the first step, the hydrolysis of hemicellulose was preferred tothat of cellulose due to higher reactivity of hemicellulose, and the major products were pentoses, namely xylose (69 %) and arabinose (6.7 %). The yield of hexoses was only 1.9 % in this

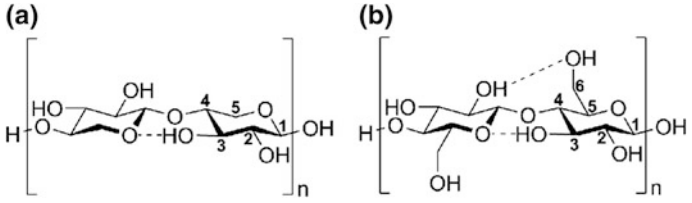

Fig. 2.16 Structures of **a** xylan and **b** cellulose. The hydrogen bond at OH group coordinating to C6 would make cellulose less reactive

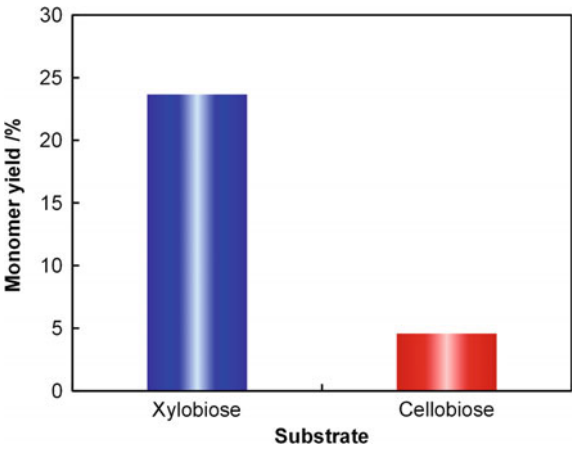

Fig. 2.17 Hydrolysis of xylobiose (the smallest model of xylan) and cellobiose (that of cellulose) by K26 at 443 K for 10 min. Legends: *blue bar* xylose and *red bar* glucose

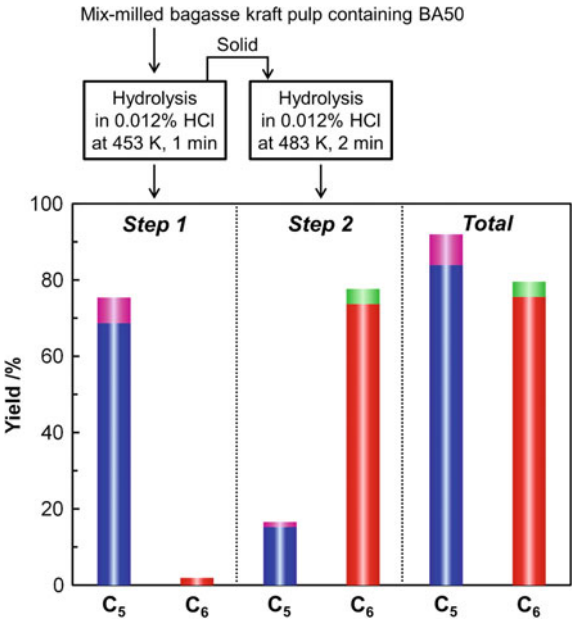

Fig. 2.18 Two-step hydrolysis of cellulose/hemicellulose in bagasse kraft pulp. Legends: *blue bar* xylose; *pink bar* arabinose; *red bar* glucose; and *green bar* fructose and mannose

step. In contrast, glucose(74 %) and other hexoses [fructose (2.5 %) and mannose (1.5 %)] from cellulose were mainly produced in the second step. The yields of xylose and arabinose in this step were only 15 % and 1.4 %, respectively.This separate production of sugars will be advantageous for their further use. The total yields of sugars in this cascade reaction were 76 % for glucose, 4.0 % for other hexoses, 84 % for xylose, and 8.1 % for arabinose.

2.3.3 *Role of Mix-Milling Pretreatment in Cellulose Hydrolysis*

In order to clarify the role of the mix-milling pretreatment, individually ball-milled cellulose and mix-milled cellulose containing K26 were analyzed by microscopes (optical microscope and SEM, Fig. 2.19). The particles of individually ball-milled cellulose were clear or white and their diameter was *ca.* 10 μm (Fig. 2.19a). Individually ball-milled K26 had black small particles (≤1 μm) (Fig. 2.19b). The particle size of mix-milled cellulose containing K26 was similar to that of individually ball-milled cellulose, whereas the surface color was black (Fig. 2.19c). The particle size distributions of both individually ball-milled and mix-milled celluloses estimated by laser diffraction were also almost the same (37–40 μm, Fig. 2.20). These results suggest that small K26 particles are attached to the surface of large cellulose particles. In fact, the SEM image of the mix-milled cellulose sample (Fig. 2.19d) showed that there were small particles on a large particle. Hence, cellulose and K26 in the mix-milled sample would have a tight contact.

The author further analyzed the mix-milled cellulose containing K26 by ^{13}C CP/MAS NMR spectroscopy and viscometry to investigate chemical properties of cellulose. As well as XRD measurement (Fig. 2.11), ^{13}C CP/MAS NMR spectroscopy indicated that both individually ball-milled and mix-milled cellulose samples were in amorphous form (Fig. 2.21). The *CrI* values determined from the

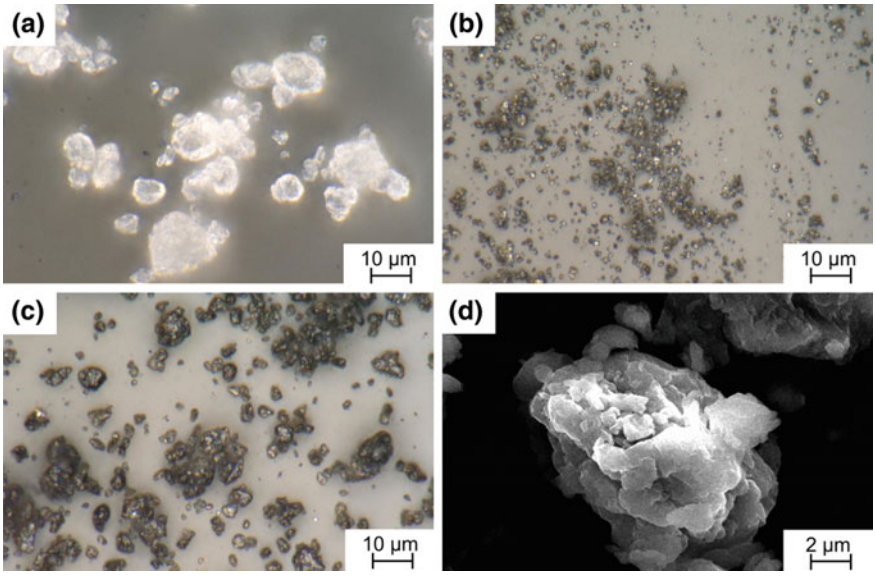

Fig. 2.19 Microscopic images of cellulose samples. Optical microscopic images of **a** individually ball-milled cellulose, **b** individually ball-milled K26, and **c** mix-milled cellulose containing K26 and **d** SEM image of the mix-milled cellulose sample

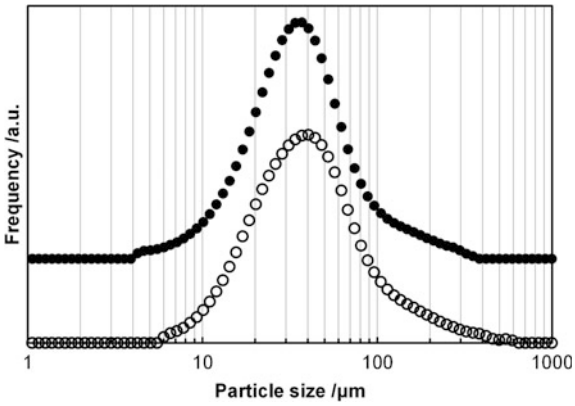

Fig. 2.20 Particle size distributions of mix-milled cellulose containing K26 (*closed circles*) and simple mixture of individually ball-milled cellulose and individually ball-milled K26 (*open circles*), which were observed by laser diffraction

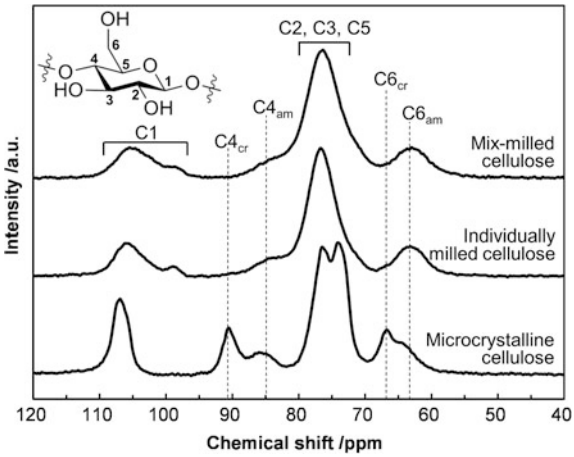

Fig. 2.21 ^{13}C CP/MAS NMR spectra of mix-milled cellulose containing K26 and individually ball-milled cellulose. $C4_{cr}$ and $C6_{cr}$ show the peaks derived from crystalline cellulose and $C4_{am}$ and $C6_{am}$ represent those from amorphous one

C4 signals based on Eq. 1.2 were less than 5 % for both samples. The DP of mix-milled cellulose was determined to be 690 by viscometry with a 9 wt% LiCl/DMAc solvent at 303 K and the Mark-Houwink-Sakurada equation (Eq. 2.4) [23].

$$[\eta] = KM_w^a \tag{2.4}$$

in which $[\eta]$ (dL g^{-1}) and M_w (g mol^{-1}) are intrinsic viscosity and weight average molecular weight, respectively. The values of K and a for cellulose in the 9 wt% LiCl/DMAc solvent at 303 K have been reported as 1.278×10^{-3} dL g^{-1} and 1.19

in a reference [23]. The value of $[\eta]$ is determined from Eq. 2.5 and experimental data (Fig. 2.22).

$$[\eta] = \lim_{c \to 0} \frac{\frac{t}{t_0} - 1}{c} \tag{2.5}$$

where c (unit: g dL^{-1}) is concentration of cellulose, t (s) is flow time of solution in a viscometer, and t_0 (s) is flow time of solvent (in this study, 9 wt% LiCl/DMAc).

The DP of mix-milled cellulose (690) was half as high as that of microcrystalline cellulose (1240), and the value was similar to that of individually milled cellulose (640). Therefore, K26 did not hydrolyze cellulose into soluble fractions during the milling process, which stood in stark contrast to H_2SO_4 [31, 33] and Amberlyst 70 (vide supra). The difference in the catalytic performance between individually ball-milled cellulose (Table 2.5, entry 26) and mix-milled cellulose (entry 35) is not ascribed to the nature of cellulose, but to the contact between the catalyst and cellulose, i.e., loose/tight contact.

To confirm the role of mix-milling pretreatment to make a tight contact between solids, the author investigated two types of model reactions: (i) cellobiose (water-soluble substrate) and K26 (insoluble catalyst) and (ii) cellulose (insoluble substrate) and benzoic acid (soluble catalyst). Even though the mix-milling pretreatment makes a tight contact between these compounds, the soluble substrate or catalyst dissolves in water to give liquid-solid reactions; in brief, the promotional effect of mix-milling should not be observed in these model reactions. Note that benzoic acid was suitable for this study employing solid-solid mixing since benzoic acid itself is solid and is a model of weakly acidic species on carbon catalysts (see Sect. 3.3.2). A typical soluble catalyst H_2SO_4 is unable to use in this model reaction, as H_2SO_4 itself is liquid and depolymerizes cellulose during the

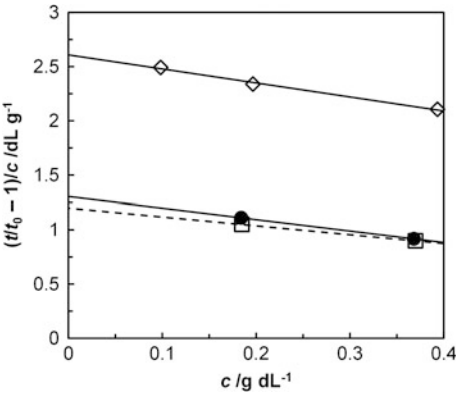

Fig. 2.22 Plots of $(t/t_{0-1})/c$ against c. In figure, the intercept is corresponding to $[\eta]$. Legends: *open diamonds* with *solid line* microcrystalline cellulose; *closed circles* with *solid line* mix-milled cellulose; and *open squares* with *dashed line* individually ball-milled cellulose

mix-milling pretreatment [31, 33]. For the combination (i), regardless of the presence/absence of mix-milling pretreatment, the hydrolysis of cellobiose by K26 proceeded at almost the same rate (Table 2.7, entries 51 and 52). Likewise, the combination (ii) showed no positive effect of mix-milling pretreatment on the hydrolysis of cellulose by benzoic acid (entries 53 and 54). In sharp contrast to these model reactions, the mix-milling pretreatment drastically accelerated the hydrolysis of solid cellulose by solid K26 and afforded *ca.* seven times higher glucan yield than individual ball-milling did (entries 35 and 55). These results suggested that the mix-milling pretreatment enhances only solid-solid reactions by forming a tight contact, but does not liquid-solid ones.

A kinetic study of the hydrolysis of cellulose was also performed to quantitatively elucidate the role of mix-milling pretreatment, in which the author chose 418 K as a reaction temperature to accurately determine kinetic parameters, as the reaction proceeds too rapidly to estimate the parameters at higher reaction temperatures such as 453 K (see Table 2.5, entry 35). Figure 2.23 shows the time course of the hydrolysis of mix-milled cellulose containing K26 in distilled water at 418 K. The amount of unreacted cellulose (black diamonds) gradually decreased with increasing reaction time. In the initial stage of the reaction, oligosaccharides (blue squares) were predominantly produced and their total yield was maximized at 6 h (44 %). After 6 h, glucose (red circles) was the major product instead of oligosaccharides. The yield of glucose increased with decrease of the yield of oligosaccharides and reached 72 % at 24 h with 97 % conversion of cellulose (Table 2.5, entry 48). This time course clearly indicates that oligosaccharides are intermediates in the reaction route from cellulose to glucose. The decomposition of

Table 2.7 Effect of solubility of substrate and catalyst on hydrolysis after mix-milling pretreatment

Entry	Pretreatment	Substrate	Catalyst	Conv./%	Yield based on carbon/%	
					Glc[a]	Olg[b]
51[c]	Milling only K26	Cellobiose	K26	12[f]	9.0	–
52[c]	Mix-milling	Cellobiose	K26	14[f]	11	–
53[d]	Milling only cellulose	Cellulose	Benzoic acid	17	3.4	9.8
54[d]	Mix-milling	Cellulose	Benzoic acid	13	2.7	8.7
55[e]	Individual milling	Cellulose	K26	18	2.9	10
35[e]	Mix-milling	Cellulose	K26	93	20	70

[a]Glucose
[b]Water-soluble oligosaccharides (DP = mainly 2–6)
[c]Conditions: cellobiose 342 mg; K26 50 mg; distilled water 40 mL; 463 K; rapid heating-cooling condition (Fig. 2.3)
[d]Conditions: cellulose 324 mg; benzoic acid 50 mg; distilled water 40 mL; 453 K; 20 min
[e]Conditions: cellulose 324 mg; K26 50 mg; distilled water 40 mL; 453 K; 20 min
[f]Conversion of cellobiose was calculated from the total amount of recovered and adsorbed cellobiose. For the estimation of adsorbed amount of cellobiose on K26, the adsorption equilibrium constant and adsorption capacity were used (see Sect. 3.3.3)

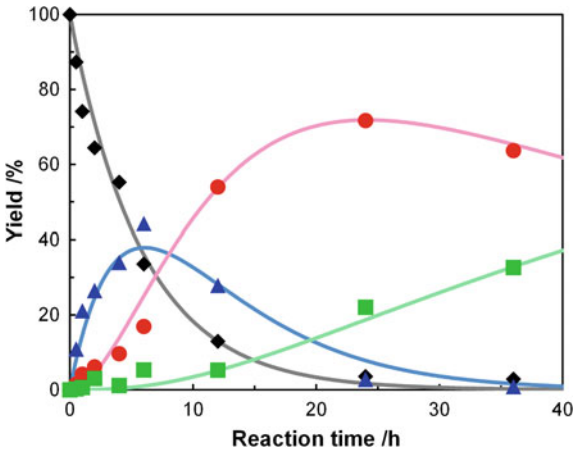

Fig. 2.23 Time course of hydrolysis of mix-milled cellulose containing K26 at 418 K. The *dots* show the experimental data and the *lines* are the results of kinetic simulations based on Eqs. 2.11–2.14. Legends: *black diamonds* cellulose; *red circles* glucose; *blue triangles* oligosaccharides; and *green squares* by-products

glucose happened to generate by-products (green triangles) after accumulation of glucose in the reaction. For these results, the hydrolysis of cellulose mainly consists of three steps as shown in Eq. 2.6 [38]: hydrolysis of cellulose to water-soluble oligosaccharides; that of oligosaccharides to glucose; and decomposition of glucose.

$$\text{Cellulose} \longrightarrow \text{Oligosaccharides} \longrightarrow \text{Glucose} \longrightarrow \text{By-products} \tag{2.6}$$

where k_1, k_2, and k_3 (unit: h^{-1}) are pseudo first-order rate constants for hydrolysis of cellulose, that of oligosaccharides, and decomposition of glucose, respectively.

The reaction rates for respective steps are represented as Eqs. 2.7–2.10, for which first-order dependence on substrates has been postulated as reported elsewhere [39–41].

$$\frac{\mathrm{d}[\text{Cellulose}]}{\mathrm{d}t} = -k_1[\text{Cellulose}] \tag{2.7}$$

$$\frac{\mathrm{d}[\text{Oligosaccharides}]}{\mathrm{d}t} = k_1[\text{Cellulose}] - k_2[\text{Oligosaccharides}] \tag{2.8}$$

$$\frac{\mathrm{d}[\text{Glucose}]}{\mathrm{d}t} = k_2[\text{Oligosaccharides}] - k_3[\text{Glucose}] \tag{2.9}$$

$$\frac{\mathrm{d}[\text{By - products}]}{\mathrm{d}t} = k_3[\text{Glucose}] \tag{2.10}$$

where [Cellulose], [Oligosaccharides], [Glucose], and [By-products] (unit: M) are concentrations of respective compounds and t (h) is reaction time. The integration of these formulae gives Eqs. 2.11–2.14.

$$[\text{Cellulose}] = [\text{Cellulose}]_0 e^{-k_1 t} \tag{2.11}$$

$$[\text{Oligosaccharides}] = [\text{Cellulose}]_0 \frac{k_1}{k_2 - k_1} \left(e^{-k_1 t} - e^{-k_2 t}\right) \tag{2.12}$$

$$[\text{Glucose}] = [\text{Cellulose}]_0 \frac{k_1 k_2}{k_2 - k_1} \left\{ \frac{1}{k_3 - k_1} \left(e^{-k_1 t} - e^{-k_3 t}\right) + \frac{1}{k_3 - k_2} \left(e^{-k_3 t} - e^{-k_2 t}\right) \right\} \tag{2.13}$$

$$[\text{By - products}] = [\text{Cellulose}]_0 - [\text{Cellulose}] - [\text{Oligosaccharides}] - [\text{Glucose}] \tag{2.14}$$

where $[\text{Cellulose}]_0$ (unit: M) is initial concentration of cellulose and $k_1 \neq k_2 \neq k_3$.

Based on Eqs. 2.11–2.14, the author simulated the time course of the hydrolysis of mix-milled cellulose containing K26. Each simulated curve (line) in Fig. 2.23 fitted well with experimental data (dots), showing the reliability of this curve fitting. The rate constants estimated from the simulation were $k_1 = 0.17\ \text{h}^{-1}$, $k_2 = 0.16\ \text{h}^{-1}$, and $k_3 = 0.017\ \text{h}^{-1}$. Surprisingly, the hydrolysis of cellulose to oligosaccharides proceeds as fast as that of oligosaccharides to glucose ($k_1/k_2 = 1.1$) in this reaction system, as the rate-determining step for glucose production is generally the depolymerization of cellulose to oligosaccharides due to insolubility and low reactivity of cellulose (i.e., $k_1/k_2 < 1$) [38]. The decomposition of glucose was approximately 10 times slower than the two hydrolysis reactions ($k_1/k_3 = 10$, $k_2/k_3 = 9.4$), resulting in high yields of glucose.

For quantitative comparison with the mix-milling pretreatment, the same analytic approach based on Eqs. 2.11–2.14 was performed for the hydrolysis of individually ball-milled cellulose by K26 at 418 K, in which a sampling method was employed to rigorously quantify the reaction products due to low reaction rates. Note that the reactivity of individually ball-milled cellulose itself should be similar to that of mix-milled cellulose (vide supra). In the hydrolysis of individually ball-milled cellulose, similar to that of mix-milled cellulose, the predominant formation of oligosaccharides was observed in the initial stage, followed by hydrolysis to glucose and successive degradation of glucose. The rate constants were determined to be $k_1 = 0.013\ \text{h}^{-1}$, $k_2 = 0.16\ \text{h}^{-1}$, and $k_3 = 0.017\ \text{h}^{-1}$ by the simulation. The value of k_1 was 13-fold diminished by changing the pretreatment method from mix-milling to individual ball-milling, while the values of k_2 and k_3 were the same regardless of the pretreatment methods. Accordingly, the ratio of k_1/k_2 in this case was only 0.018, exhibiting that the rate-determining step for glucose formation was the hydrolysis of solid cellulose to soluble oligosaccharides. Therefore, the author

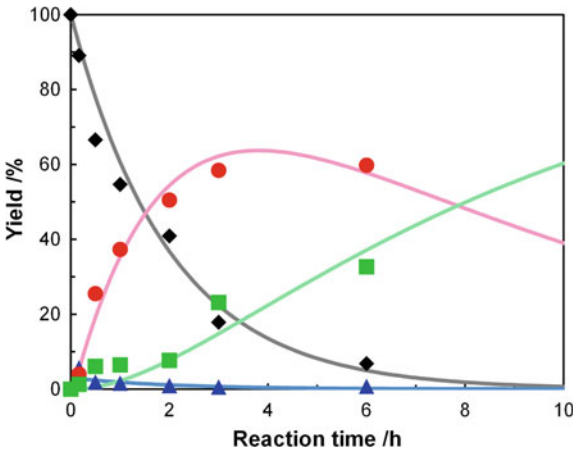

Fig. 2.24 Time course of hydrolysis of individually ball-milled cellulose by H_2SO_4 (50 mM) at 418 K. The *dots* show the experimental data and the *lines* are the results of kinetic simulations based on Eqs. 2.11–2.14. Legends: *black diamonds* cellulose; *red circles* glucose; *blue triangles* oligosaccharides; and *green squares* by-products

has quantitatively revealed that the mix-milling pretreatment selectively and drastically accelerated the solid-solid reaction.

A typical soluble acid catalyst H_2SO_4 was also tested in the hydrolysis of individually ball-milled cellulose in order to compare solid–solid and solid–liquid reactions (Fig. 2.24). In this test, 50 mM (0.49 wt%) of H_2SO_4 has been employed, as this concentration is a usual value in diluted H_2SO_4 processes [9, 10, 42]. The kinetic simulation provided the rate constants, i.e., $k_1 = 0.5\ h^{-1}$, $k_2 = 17\ h^{-1}$, and $k_3 = 0.12\ h^{-1}$. As previously reported [38], the hydrolysis of solid cellulose to soluble oligosaccharides was significantly slower than that of oligosaccharides ($k_1/k_2 = 0.029$). Consequently, the high ratio of k_1/k_2 provided by mix-milling cellulose with K26 is specific to this new pretreatment method to form a tight solid–solid contact.

2.4 Conclusions

Simple carbon materials catalyze hydrolysis of cellulose, and their catalytic activities correlate with the amounts of weakly acidic OFGs. Such weak acid catalysts can survive even in the presence of buffer and salt potentially derived from real biomass. However, at issue is a loose contact between the solid substrate and solid catalyst, limiting the yield of glucose at most 36 % even when using the most active catalyst, the alkali-activated carbon K26. This obstacle has been overcome by the new pretreatment method, namely mix-milling cellulose and K26 to make a tight solid–solid contact. The hydrolysis of mix-milled cellulose provides 72 % yield of

glucose in distilled water and 88 % yield with 90 % selectivity in the trace HCl solution, which is one of the highest glucose yields ever reported. The mix-milling pretreatment is also effective for the depolymerization of cellulose/hemicellulose in bagasse kraft pulp, resulting in 80 and 92 % yields of hexoses and pentoses, respectively. Characterization of mix-milled cellulose, a series of model reactions, and kinetic studies clearly show that the hydrolysis of water-insoluble cellulose to soluble oligosaccharides over the carbon catalyst is selectively and drastically accelerated owing to the tight contact between solid cellulose and solid K26 created by the mix-milling pretreatment.

Based on this study, Fukuoka et al. have designed an attractive recycling system for saccharification of raw biomass [43]. In their work, a carbon catalyst named *E-Carbon* has been prepared by carbonizing and oxidizing *Eucalyptus* under air and has been used for mix-milling pretreatment with *Eucalyptus*, followed by hydrolysis; that is, *Eucalyptus* is a substrate as well as a carbon source in this process. The solid residue after the reaction contain both *E-Carbon* and remaining substrate and can be utilized as a carbon catalyst again after carbonization and oxidation, making this process practicable to build up sustainable societies.

Also, it has been reported that the mix-milling pretreatment is effective for hydrolytic hydrogenation of cellulose to sorbitol by carbon-supported metal catalysts since the first step is the same hydrolysis of insoluble cellulose to soluble oligosaccharides [44, 45]. Mix-milling is a promising method to overcome a fundamental problem of solid–solid reactions, namely loose contact between solids, by making tight contact. This pretreatment method is expected to be applicable to other solid–solid reactions, e.g., oxidation of diesel soot particulates over solid catalysts [46].

References

1. Rinaldi R, Schüth F (2009) Design of solid catalysts for the conversion of biomass. Energy Environ Sci 2(6):610–626
2. Alonso DM, Bond JQ, Dumesic JA (2010) Catalytic conversion of biomass to biofuels. Green Chem 12(9):1493–1513
3. Gallezot P (2012) Conversion of biomass to selected chemical products. Chem Soc Rev 41 (4):1538–1558
4. Tuck CO, Pérez E, Horváth IT, Sheldon RA, Poliakoff M (2012) Valorization of biomass: deriving more value from waste. Science 337(6095):695–699
5. Besson M, Gallezot P, Pinel C (2013) Conversion of biomass into chemicals over metal catalysts. Chem Rev 114(3):1827–1870
6. Yabushita M, Kobayashi H, Fukuoka A (2014) Catalytic transformation of cellulose into platform chemicals. Appl Catal B Environ 145:1–9
7. Corma A, Iborra S, Velty A (2007) Chemical routes for the transformation of biomass into chemicals. Chem Rev 107(6):2411–2502
8. Serrano-Ruiz JC, West RM, Dumesic JA (2010) Catalytic conversion of renewable biomass resources to fuels and chemicals. Annu Rev Chem Biomol Eng 1:79–100
9. Kobayashi H, Fukuoka A (2013) Synthesis and utilisation of sugar compounds derived from lignocellulosic biomass. Green Chem 15(7):1740–1763

10. Rinaldi R, Schüth F (2009) Acid hydrolysis of cellulose as the entry point into biorefinery schemes. ChemSusChem 2(12):1096–1107
11. Kobayashi H, Ohta H, Fukuoka A (2012) Conversion of lignocellulose into renewable chemicals by heterogeneous catalysis. Catal Sci Technol 2(5):869–883
12. Schüth F, Rinaldi R, Meine N, Kälström M, Hilgert J, Rechulski MDK (2014) Mechanocatalytic depolymerization of cellulose and raw biomass and downstream processing of the products. Catal Today 234:24–30
13. Kobayashi H, Komanoya T, Hara K, Fukuoka A (2010) Water-tolerant Mesoporous-Carbon-Supported ruthenium catalysts for the hydrolysis of cellulose to glucose. ChemSusChem 3(4):440–443
14. Komanoya T, Kobayashi H, Hara K, Chun W-J, Fukuoka A (2011) Catalysis and characterization of carbon-supported ruthenium for cellulose hydrolysis. Appl Catal A Gen 407(1):188–194
15. Suganuma S, Nakajima K, Kitano M, Yamaguchi D, Kato H, Hayashi S, Hara M (2008) Hydrolysis of cellulose by amorphous carbon bearing SO_3H, COOH, and OH groups. J Am Chem Soc 130(38):12787–12793
16. Onda A, Ochi T, Yanagisawa K (2008) Selective hydrolysis of cellulose into glucose over solid acid catalysts. Green Chem 10(10):1033–1037
17. Mo X, López DE, Suwannakarn K, Liu Y, Lotero E, Goodwin JG Jr, Lu C (2008) Activation and deactivation characteristics of sulfonated carbon catalysts. J Catal 254(2):332–338
18. Chung P-W, Charmot A, Olatunji-Ojo OA, Durkin KA, Katz A (2013) Hydrolysis catalysis of *Miscanthus* xylan to xylose using weak-acid surface sites. ACS Catal 4(1):302–310
19. Charmot A, Chung P-W, Katz A (2014) Catalytic hydrolysis of cellulose to glucose using weak-acid surface sites on postsynthetically modified carbon. ACS Sustainable Chem Eng 2 (12):2866–2872
20. Jun S, Joo SH, Ryoo R, Kruk M, Jaroniec M, Liu Z, Ohsuna T, Terasaki O (2000) Synthesis of new, nanoporous carbon with hexagonally ordered mesostructure. J Am Chem Soc 122 (43):10712–10713
21. Sluiter A, Hames B, Ruiz R, Scarlata C, Sluiter J, Templeton D, Crocker D. Determine of structural carbohydrates and lignin in biomass: Laboratory Analytical Procedures (LAP). (Online) http://www.nrel.gov/biomass/pdfs/42618.pdf Accessed 31 Oct 2015
22. Boehm H (1994) Some aspects of the surface chemistry of carbon blacks and other carbons. Carbon 32(5):759–769
23. McCormick CL, Callais PA, Hutchinson BH Jr (1985) Solution studies of cellulose in lithium chloride and *N,N*-dimethylacetamide. Macromolecules 18(12):2394–2401
24. Strlič M, Kolenc J, Kolar J, Pihlar B (2002) Enthalpic interactions in size exclusion chromatography of pullulan and cellulose in LiCl-*N,N*-dimethylacetamide. J Chromatogr A 964(1):47–54
25. Mäurer T, Müller SP, Kraushaar-Czarnetzki B (2001) Aggregation and peptization behavior of zeolite crystals in sols and suspensions. Ind Eng Chem Res 40(12):2573–2579
26. Gopalakrishnan S, Yada S, Muench J, Selvam T, Schwieger W, Sommer M, Peukert W (2007) Wet milling of H-ZSM-5 zeolite and its effects on direct oxidation of benzene to phenol. Appl Catal A Gen 327(2):132–138
27. Mitra B, Kunzru D (2008) Washcoating of different zeolites on cordierite monoliths. J Am Ceram Soc 91(1):64–70
28. Bobleter O (1994) Hydrothermal degradation of polymers derived from plants. Prog Polym Sci 19(5):797–841
29. Strachan J (1938) Solubility of cellulose in water. Nature 141:332–333
30. Fang Z, Koziński JA (2000) Phase behavior and combustion of hydrocarbon-contaminated sludge in supercritical water at pressures up to 822 MPa and temperatures up to 535 ºC. Proc Combust Inst 28(2):2717–2725
31. Shrotri A, Lambert LK, Tanksale A, Beltramini J (2013) Mechanical depolymerisation of acidulated cellulose: understanding the solubility of high molecular weight oligomers. Green Chem 15(10):2761–2768

32. Hick SM, Griebel C, Restrepo DT, Truitt JH, Buker EJ, Bylda C, Blair RG (2010) Mechanocatalysis for biomass-derived chemicals and fuels. Green Chem 12(3):468–474
33. Meine N, Rinaldi R, Schüth F (2012) Solvent-free catalytic depolymerization of cellulose to water-soluble oligosaccharides. ChemSusChem 5(8):1449–1454
34. Geboers J, Van de Vyver S, Carpentier K, Jacobs P, Sels B (2011) Efficient hydrolytic hydrogenation of cellulose in the presence of Ru-loaded zeolites and trace amounts of mineral acid. Chem Commun 47(19):5590–5592
35. International Chemical Information Service (ICIS). Hydrochloric acid prices, markets & analysis. (Online) http://www.icis.com/chemicals/hydrochloric-acid/ Accessed 31 Oct 2015
36. Nexant. Sulfur/sulfuric acid market analysis. (Online) http://yosemite.epa.gov/oa/eab_web_docket.nsf/Filings%20By%20Appeal%20Number/EFAE40E5FFEFBBF785257A2A0047AC45/$File/Exhibit%2052m%20to%20Revised%20Petition%20for%20Review%20…12.52m.pdf Accessed 31 Oct 2015
37. Maréchal Y, Chanzy H (2000) The hydrogen bond network in I_β cellulose as observed by infrared spectrometry. J Mol Struct 523(1):183–196
38. Abatzoglov N, Bouchard J, Chornet E, Overend RP (1986) Dilute acid depolymerization of cellulose in aqueous phase: Experimental evidence of the significant presence of soluble oligomeric intermediates. Canad J Chem Eng 64(5):781–786
39. Saeman JF (1945) Kinetics of wood saccharification—hydrolysis of cellulose and decomposition of sugars in dilute acid at high temperature. Ind Eng Chem 37(1):43–52
40. Sasaki M, Kabyemela B, Malaluan R, Hirose S, Takeda N, Adschiri T, Arai K (1998) Cellulose hydrolysis in subcritical and supercritical water. J Supercrit Fluids 13(1):261–268
41. Kobayashi H, Ito Y, Komanoya T, Hosaka Y, Dhepe PL, Kasai K, Hara K, Fukuoka A (2011) Synthesis of sugar alcohols by hydrolytic hydrogenation of cellulose over supported metal catalysts. Green Chem 13(2):326–333
42. Faith WL (1945) Development of the Scholler process in the United States. Ind Eng Chem 37 (1):9–11
43. Kobayashi H, Kaiki H, Shrotri A, Techikawara K, Fukuoka A (2016) Hydrolysis of woody biomass by biomass-derived reusable heterogeneous catalyst. Chem Sci 7(1):692–696
44. Komanoya T, Kobayashi H, Hara K, Chun W-J, Fukuoka A (2014) Kinetic study of catalytic conversion of cellulose to sugar alcohols under low-pressure hydrogen. ChemCatChem 6(1):230–236
45. Liao Y, Liu Q, Wang T, Long J, Zhang Q, Ma L, Liu Y, Li Y (2014) Promoting hydrolytic hydrogenation of cellulose to sugar alcohols by mixed ball milling of cellulose and solid acid catalyst. Energy Fuels 28(9):5778–5784
46. Stanmore BR, Brilhac JF, Gilot P (2001) The oxidation of soot: a review of experiments, mechanisms and models. Carbon 39(15):2247–2268

http://www.springer.com/978-981-10-0331-8

A Study on Catalytic Conversion of Non-Food Biomass into Chemicals
Fusion of Chemical Sciences and Engineering
Yabushita, M.
2016, XVII, 158 p. 101 illus., 58 illus. in color.,
Hardcover
ISBN: 978-981-10-0331-8